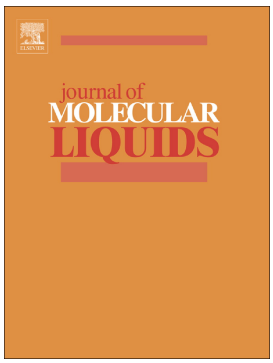

Study of heavy metals biosorption on native and alkali-treated apricot shells and its application in wastewater treatment

Tatjana D. Šoštarić, Marija S. Petrović, Ferenc T. Pastor, Davor R. Lončarević, Jelena T. Petrović, Jelena V. Milojković, Mirjana D. Stojanović

PII: S0167-7322(18)30701-3
DOI: doi:10.1016/j.molliq.2018.03.055
Reference: MOLLIQ 8829

To appear in: *Journal of Molecular Liquids*

Received date: 8 February 2018
Revised date: 13 March 2018
Accepted date: 14 March 2018

Please cite this article as: Tatjana D. Šoštarić, Marija S. Petrović, Ferenc T. Pastor, Davor R. Lončarević, Jelena T. Petrović, Jelena V. Milojković, Mirjana D. Stojanović , Study of heavy metals biosorption on native and alkali-treated apricot shells and its application in wastewater treatment. The address for the corresponding author was captured as affiliation for all authors. Please check if appropriate. Molliq(2017), doi:10.1016/j.molliq.2018.03.055

Study of heavy metals biosorption on native and alkali-treated apricot shells and its application in wastewater treatment

Tatjana D. Šoštarić*[a], Marija S. Petrović[a], Ferenc T. Pastor[b,c], Davor R. Lončarević[d], Jelena T., Petrović[a], Jelena V. Milojković[a], Mirjana D. Stojanović[a]

[a] *Institute for Technology of Nuclear and Other Mineral Raw Materials, Franchet d'Esperey 86, 11000 Belgrade, Serbia*

[b] *University of Belgrade, Faculty of Chemistry, Studentski trg 12-16, 11000 Belgrade, Serbia;*

c Ghent University Global Campus, 119 Songdomunhwa-Ro, Yeonsu-Gu, Incheon, South Korea

[d] *University of Belgrade, Institute of Chemistry, Technology and Metallurgy, Department of Catalysis and Chemical Engineering, Njegoševa 12, 11000 Belgrade, Serbia*

*****Corresponding author. Tel.: +381 11 3691 722

Email address: t.sostaric@itnms.ac.rs (T. D. Šoštarić)

Abstract

Locally available apricot (*Prunus armeniaca* L.) shells classified as a waste product from fruit processing, were alkali activated in order to develop an efficient heavy metal ions sorbent for water purification. To examine the changes occurred after alkali treatment, raw (SH) and modified apricot shells (SHM) were thoroughly characterized in terms of their chemical composition and surface properties. Chemical analysis revealed that alkaline treatment causes the disintegration of hemicellulose (its content decreased from 19.2 to 3.5 %), which was in accordance with FTIR results. SEM micrographs and the mercury intrusion porosimetry revealed a larger surface area and porosity of SHM. Bohem's acid-base titration method indicated that the most of the SHM surface carboxylic groups were in sodium salt form and together with the pH of points of zero charge showed increase of surface alkalinity after modification. Treatment with NaOH enhanced the adsorption capacity by 154, 61 and 90 % for Cu^{2+}, Zn^{2+} and Pb^{2+}, respectively. The amount of cations released from SHM was almost equal to the amount of adsorbed metal ions, suggesting ion exchange mechanism. The pseudo-second order kinetic indicated that the heavy metals cations were bound predominantly by complexation.

In order to establish the effectiveness of the biosorbent in real wastewater sample, SHM was employed for cleaning-up of drain water emanating from atomic adsorption spectrophotometer. The SHM showed high removal efficiency towards multiple metal ions. The amounts of Fe, Pb, Cu and Cr ions were reduced by 97, 87, 81 and 80 %, respectively, while Ni and Zn amounts were reduced for 33 and 14 %.

Used biosorbent SHM can be successfully regenerated with HCl (desorption > 95 %) and after regeneration biosorbent can be reused or it can be safely disposed.

Kew words: apricot shells, waste minimization, characterisation, heavy metals removal, wastewater treatment

1. Introduction

From environmental and economic point of view the most appropriate and therefore the most common biomasses used for the biosorption process are waste biomaterials or agricultural

by-products. It is possible to extract some valuable compounds from organic waste such as pectine, fibers, antioxidants etc., but often vast quantities of lignocellulose fraction stay unused [1]. In order to minimize lignocellulosic waste a number of such materials have been investigated as adsorbents for the removal of heavy metals from the wastewaters: either in its native form [2,3], treated form [4,5,6], or in active carbon form [7,8,9]. Removal of heavy metals from aqueous solution by lignocellulosic materials is provided by the presence of various functional groups on their surface (hydroxyl, carbonyl, phosphate, amino and thiol groups plays a major role in heavy metals binding mechanism). However, the presence of the functional groups on the surface of biomaterials can't guarantee efficient removal of heavy metal ions, because the biosorption process is affected by various factors such as the number of active sites, their accessibility, their chemical state and their affinity for the targeted metal. Therefore, it can be concluded that biosorption efficiency depends largely on the type of biomass.

The advantage of lignocellulosic materials usage for the treatment of wastewater is that cellulose (that mostly dominates in the composition of these materials) has good chemical stability and mechanical strength due to its crystal structure. However, cellulose has a limited number of free hydroxyl groups which are available for metal ions binding. This is because mostly these groups are involved in the formation of a large number of inter- and intramolecular hydrogen bonds. According to Abdolali et al. [10], in lignocellulosic materials the majority of cellulose (65 %) is represented by highly organized crystal lattice that is not available to molecules of water and other solvents, while the minor parts are linked to hemicellulose (20 – 40 %) and lignin (15 - 25%). Application of lignocellulosic materials for biosorption process has additional disadvantages, such as low biosorption capacity and the release of organic components in to the solution. Therefore, such materials need to be subject of modification. In that way, soluble organic compounds are extracted and the adsorption performances are improved, which justifies the cost of a pretreatment.

In this paper, apricot shells were chosen because they fulfil the most important criteria of unconventional biosorbent: they are cheap and abundant waste. Apricots have an important role in Serbian fruit production with average annual production of 30,000 t that generates more than 1,800 t of waste [11]. Although, apricot shells can be used in the pharmaceutical industry and in the manufacture of abrasive powders, there is no systematized collection and use of this type of

waste. Since it is usually incinerate or dispose of in landfills, elimination and re-use of it would contribute appreciably to the waste or ash disposal issues.

It is important to mention that the apricot shells, so far were used exclusively in the form of activated carbon [7,12,13] in biosorption experiments, not in its natural or alkali modified form.

In the following paper the physical and chemical properties of raw (SH) and alkali treated apricot shells (SHM) have been determined and compared, in order to investigate their potential to remove heavy metal ions (Cu^{2+}, Zn^{2+} and Pb^{2+}) from aqueous solution. Also, for the first time, biosorbent (SHM) was applied for cleaning up drained water of atomic adsorption spectrophotometer.

2. Materials and methods

2.1 Biomass preparation

2.1.1 Untreated biomass (SH)

Apricot stones (*Prunus armeniaca* L.) were obtained from Juice Factory "Vino Župa" Aleksandrovac, located in the Rasina District of Serbia. Apricot stones were air dried at room temperature. The shells were manually separated from seeds. Only apricot shells (SH) were used for studies. The samples were washed with deionized water, dried at 50 $^{\circ}$C for 24 h, grinded (KHD Humbolt Wedag AG, Germany) and sieved into particle size less than 0.3 mm.

2.1.2 Treated biomass (SHM)

Treatment was conducted by soaking SH powder in 1.0 mol/L NaOH solution in a 1:20 solid-to-liquid ratio (g/mL). Suspension was allowed to stir for 180 min at 25 $^{\circ}$C on magnetic stirrer at 250 rpm. The samples were washed with deionized water until it gave no colour and the pH of filtrate was close to neutral. After drying (at 50 $^{\circ}$C for 24 h) the sample was stored in plastic containers.

2.2 Metal solution preparation

Initial solutions of selected heavy metals (Cu^{2+}, Zn^{2+} and Pb^{2+}) with a concentration of 1000 mg/L, were prepared by dissolving $Cu(NO_3)_2 \times 3H_2O$; $ZnSO_4 \times 7H_2O$ and $Pb(NO_3)_2$ (Analytical grade) in deionized water. In order to obtain the desired concentration of experimental solutions, the initial solution was diluted with deionized water.

2.3 Physical and chemical characterization of SH and SHM

Ash and moisture contents of both samples were determined based on the ASTM standard methods ASTM E871-82 (2013) and ASTM E1755-01 (2015).

Quantification of the amount of lignin, holocellulose, cellulose and hemicellulose: The procedure is based on the gradual removal of components one by one from the samples. First step is removal of compounds which may interfere with some analyses, like waxes, fats, resins, gums, sugars, starches, pitch, sterols, flavonoids, tannins, terpenes, quinones, chlorophyll and others [14]. Extraction of above-mentioned compounds was conducted in 100 mL Erlenmayer flasks with attached reflux condenser, by soaking the biomass (1.0 g) in 44 mL of acetone. The flask was partially immersed in a constant temperature water bath set at 58 $^{\circ}$C and it was left to stir for 3 h. The suspension was filtered through pre-weighed sintered glass funnel, than washed with 10 mL of acetone, followed by distilled water. The residue was dried at 105 $^{\circ}$C for 24 h and the amount of extractive was determined gravimetrically. **The lignin content** in extractive-free samples was determined using TAPPI standard method [15]. In order to quantify **the amount of holocellulose** experiments were conducted in 250 mL Erlenmeyer flasks (with attached reflux condenser) by adding 5 mL of 0.7 % $NaClO_2$ in mixture of biomass (1.0 g) and distilled water (50 mL). The pH was adjusted to 4.0 with acetic acid. The suspension was placed on a hot plate and boiled for 2 h at 75 $^{\circ}$C. The mixture was then cooled down and filtered through pre-weighed sintered glass funnel, washed with water (750 mL) followed by 250 mL 2% $NaHSO_3$ and after that, once more with water (1000 mL). The residue was dried at 105 $^{\circ}$C for 24 h and the amount of holocellulose was determined gravimetrically. In order to determine **the cellulose content** the holocellulose residue (1.0 g) was immersed in 35 mL of 17.5 % NaOH solution and left for a 10 min at room temperature. Thereafter another 40 mL of the same solution was added and obtained

mixture was left for 35 more min. The suspension was filtered through pre-weighed sintered glass funnel and washed with distilled water (750 mL). Afterwards, the sample was immersed in 15 mL of 10 % acetic acid for 10 min. After filtration it was washed with 750 mL of distilled water. Next 15 mL of 0.5 % $NaHCO_3$ was added to suspension, followed by hot water washing until filtrate was neutral. The cellulose content as the remaining residue was determined gravimetrically. **The hemicellulose content** of the samples was determined by subtracting of cellulose content from holocellulose [16].

Elemental analysis (C, H, N and S) of samples was performed using "Vario-EL III; CHNS-O Elementar Analyzer" (Hanau, Germany). Operating ranges varied between the elements: 0.03–20 mg for C; 0.03–3.0 mg for H; 0.03–2.0 mg for N and 0.03–6.0 mg for S. Oxygen content were obtained by subtracting the sum of the obtained elemental values from 100 %.

The point of zero charge (pH*pzc*) was determined using method described by Milonjić et al. [17].

The surface structure of SH and SHM were analyzed by Scanning Electron Microscopy (SEM) coupled with energy dispersive X-ray analysis (EDX) after coating of samples with a thin layer of gold. SEM-EDX analysis was performed using a JEOL JSM-6610 LV SEM model. Pore size, pore volume distribution, and porosity were determined by mercury intrusion porosimetry on Pascal 140/440, Thermo Scientific.

The concentrations of acidic and basic sites on SH and SHM were determined by the method proposed by Boehm [18] as well as by the direct potentiometric titrations. Determination of acidic sites was based on utilization of the following solutions: 0.05 M NaOH (for determination of total acidic sites), Na_2CO_3 (for determination of carboxylic and lactonic sites) and $NaHCO_3$ (for determination of carboxylic sites). Experiments were performed by soaking 1.0 g of biomass in 50 mL of each solution and stirring for 24 h on a shaker at room temperature. Suspensions were filtered and supernatants were titrated with standard solutions of 0.05 M HCl solution. The concentration of the hydroxylic sites were calculated by subtracting the concentrations of the carboxylic and lactonic sites from the total acidic sites concentration while the concentrations of lactonic sites were calculated by subtracting the concentrations of carboxylic sites from the results obtained for carboxylic and lactonic sites. The basic sites were neutralized using a 0.05 M HCl solution and after filtration supernatans were titrated with

standard solutions of 0.05 M NaOH. The point at which the second derivative crosses zero is taken as the end point of the titration.

Direct potentiometric titrations of SH and SHM were performed by mixing 1.5 g of SH or SHM with 30 mL of deionized water and titrated with 0.3 M solutions of HCl or NaOH. After addition of each aliquot titration mixture was left for 8 minutes in order to let the pH to reach equilibrium value before recording. During titrations, titrated mixtures were stirred and purged with pure nitrogen (99.999 %, Messer Tehnogas AD, Serbia). Titrations were followed by 7110 pH meter with SenTix 82 electrode, WTW, Germany.

The determination of surface functional groups in samples was performed by Attenuated Total Fourier Transform Infrared Spectroscopy using Thermo Nicolet 6700 FTIR. The spectra were recorded by averaging 32 scans from 4000-400 cm^{-1}. The region between 1900 and 2200 cm^{-1} is interrupted due to strong diamond IR absorption.

Cation exchange capacity (CEC) was determined by method involves saturation of the cation exchange sites by ammonium acetate [19]. The samples (0.2 g) were added in 100 mL of 1.0 mol/L ammonium acetate and then were shaken for 120 minutes at speed of 250 rpm on orbital shaker. As a control, the same procedure was done mixing the same amount of samples with 100 mL of deionized water. The samples were filtrated and the concentrations of exchangeable cations (K^+, Na^+, Ca^{2+} and Mg^{2+} ions) released from SH and SHM in filtrates were determined by atomic adsorption spectrophotometer (Perkin Elmer AAnalyst 300).

2.4 Adsorption experiments

Adsorption experiments were conducted in a batch system by adding a precise amount of sample in 50 mL of solutions with known initial concentration of Cu^{2+}, Zn^{2+} and Pb^{2+}. The mixtures were shaken at 250 rpm and after certain period of time they were filtered and the concentration of metal ions in supernatants were determined by atomic adsorption spectrophotometer.

The removal of metal ions was investigated as a function of operating parameters such as pH value (2.0 – 6.0), initial biosorbent concentration (2 – 10 g/L), contact time (1 – 120 min), temperature of 25 $^{\circ}C$ and initial metal concentration (6 - 120 mg/L). The obtained data were used

to calculate the biosorption capacity of SH and SHM for selected metals by using the following equation:

$$q_e = \frac{V(C_i - Ce)}{m} \quad (1)$$

q - the amount of adsorbed metal ions (mg/g);

C_i and C_e - the initial and equilibrium metal concentrations (mg/L), respectively;

V - the solution volume (L);

m - the sample mass (g).

All sorption experiments were performed in triplicate. The nonlinear coefficient of determination (R^2) and the chi-square test were used as a test for goodness of fit. Chi-square test was determined as described elsewhere [20].

2.5 Kinetic study

In order to reveal nature of the sorption process all experimental date were evaluated not only by using isotherm models, but also kinetic models. Pseudo-first-order [21] and pseudo-second-order [22] as reaction based models and Weber-Morris model [23] as diffusion model were applied to the experimental data. Table 1 summarize models and equations used in this paper.

Table 1 Models used for evaluation of heavy metals sorption onto SH and SHM

2.6 Desorption study

Regeneration and reuse of exhausted SHM were performed alternately in three cycles. Regeneration of metal loaded SHM was carried out using 0.1 mol/L HCl, while adsorption experiments were done at optimum parameters (pH = 5.0; biosorbent concentration was 2 g/L; contact time was 120 min and initial metal concentration was 60 mg/L for Cu(II) and Zn(II) and 200 mg/L for Pb(II)). After each set of experiments the samples were centrifuged and metal contents were analysed by atomic adsorption spectrophotometer. Desorption efficiency calculation were previously described [28].

3 Results and discussions

3.1 Characterization of SH and SHM

3.1.1 Chemical composition and surface properties

In order to determine the changes that have occurred as a result of the alkaline treatment, comparative characterization of SH and SHM were carried out. The results of characterization of both samples are presented in Table 2.

Table 2 Physical and chemical properties of SH and SHM

The percentage of hemicellulose, lignin and cellulose present in the SH are 19.23, 22.72 and 55.23 %, respectively. However, when the raw biomass is subjected to an alkaline treatment, it is evident that there is a significant decrease in percentage of hemicellulose (3.52 %) and slight decrease in percentage of lignin (21.21 %) and increase in percentage of cellulose (57.23 %). During alkali treatment the hemicellulose is hydrolysed and the lignin is partially depolymerised due to breaking of the α-either bonds between lignin and hemicellulose [29,30]. Also, this treatment results in removal of some degradation products (weight loss after treatment was 16 %). Similar results were obtained by Ben Sghaier et al. [30] when the agava fiber (*Agava americana* L.) were treated with 1.0 mol/L NaOH. Lin et al. [31], showed that the cellulose content has increased and hemicellulose content has decreased after corn was subject to treatment with 1.5 M NaOH.

Elemental analysis results showed that SH is mainly composed of carbon (47.6%) and oxygen (46.03 %). The hydrogen content was 6.24 %, nitrogen content was 0.12 % and there was no sulphur. The obtained results are in accordance with the results obtained by researchers Demiral and Kul [32] who also investigated the element composition of apricot shells. After modification the content of the C, O, N and H in SHM has been slightly changed compared to starting sample: there was a slight decrease in carbon content (from 47.61 to 46.05 %) and slight increase in hydrogen (from 6.24 to 6.52 %) and oxygen content (from 46.03 to 47.43 %).

Changes in the elemental composition of SH and SHM are rather small, but significant. Since alkali treatment breaks the covalent bond between lignocellulose components, causing the hemicellulose hydrolysis and lignin depolymerization [33] it can cause decrease of carbon content. Increase in hydrogen content can be explained by the fact that alkali treatment affects swelling of cellulose, breaking of hydrogen bonds and formation of new one (reorganization of the crystal lattice) [34]. Change in oxygen content is due to changes in the content of other components. The obtained results were comparable to those obtained by Asadi et al. [35] treating rice bran with NaOH.

Mercury porosimetry was used to determine whether the alkali treatment increased specific surface area and porosity of biomaterial. As can be seen from obtained results presented in Table 2, alkali treatment led to an improvement of porous structure of SH. After treatment, there was a slight increase in porosity (from 25 % in SH to 30 % in SHM) and total pore volume (from 218 in SH to 271 mm^3/g in SHM) due to partial dissolution of some components like hemicellulose - leaving hollow spaces in those places. Also, specific surface area of SHM (20 m^2/g) is noticeably larger compared to untreated one (15 m^2/g), because treatment with NaOH removes natural fats and waxes from biomass surface [36] which increases effective specific surface area available for contact.

3.1.2 SEM analysis

In order to get better insight of complex nature of apricot endocarp, the SEM micrographs of outer, inner and the layer between them were taken and presented in Fig. 1. Noticeable differences in the morphology of the inner smooth and glossy layer (Fig. 1a,b), exterior rough layer (Fig. 1e,f) and cross-section of endocarp (Fig. 1c,d) have been observed. As can be seen from micrographs, pores are visible only in the Fig. 1c,d revealing that the endocarp's inside is porous. There are two types of visible pores: bigger - pore diameter is approximately 10 to 20 μm and smaller - pore diameter is approximately 1 μm.

Fig. 1 *SEM micrographs of endocarp: inner layer magnified 1000x (a), 5000x (b); cross section magnified 1000x (c), 5000x (d); exterior layer magnified 1000x (e), 5000x (f)*

In order to see if mechanical and alkaline treatment have effect on the initial porous structure of biomaterial, the SEM micrographs of milled (Fig. 2a) and afterwards alkali treated material (Fig. 2b) were taken.

Fig. 2 *SEM micrographs of: SH (a) and SHM (b); EDX spectrums of: SH (c) and SHM (d)*

As can be seen from Fig. 2a, after grinding the pores have been collapsed. Possible explanation is that after grinding, pores are clogged due to compression of material during milling. However, after the alkaline treatment, it is clearly observed that the pores are still present (Fig. 2b). Alkali treatment not only rinses the residual material left on the sample, but also dissolves some components from the material (mainly hemicelluloses, waxes and fats) [37]. Such a change makes surface of SHM more accessible to metal ions, by providing a larger contact area and more binding sites for ions, in comparison to the SH. Similar results were obtained when the olive tree pruning were treated with 1.0 mol/L NaOH [38,39]. In addition, the SEM micrographs of SHM after adsorption of metals are presented in supplementary material (Fig. 3). It is evident that the adsorption of Cu(II), Zn(II) and Pb(II) ions causes partial disruption in surface morphology of SHM, due to interaction with metal ions.

Figure 2c and 2d, shows EDX spectrum of SH and SHM, respectively. The peaks of gold are present due to sample preparation. The spectrum revealed the presence of potassium ions on surface of natural (SH) and presence of sodium ions on surface of treated material (SHM). Therefore, it can be concluded that after modification, sodium ions are bounded to the SHM.

3.1.3 The point of zero charge

In order to consider if alkaline modification changed surface charge of starting sample, the determination of pH*pzc* of the both SH and SHM samples was investigated. The value of pH*pzc* provides insight into electrostatic interactions among sorbent and metal species in solution: at pH < pH*pzc*, the surface charge is positive and may possibly interact with negative species, while at pH > pH*pzc* the surface charge is negative and may possibly interact with positive species in solution [40]. Apparently, the value of pH*pzc* is very similar for each KNO_3 concentrations indicating that SH and SHM are independent on the ionic strength of this

electrolyte. As can be seen from Fig. 3 the pH*pzc* was found to be 4.9 and 5.7 for SH and SHM, respectively. The obtained results confirmed that alkaline treatment of SH increases the pH*pzc* and surface alkalinity of modified material SHM.

Fig. 3 *pH final (pH_f) as a function of pH initial (pH_i) for SH and SHM, for different ions strengths* ■ *[KNO_3] = 0.01 mol/L;* ● *[KNO_3] = 0.1 mol/L and* ▲*[KNO_3] = 0.001 mol/L*

3.1.4 Determination of the concentrations of acidic and basic sites

Chemical heterogeneity of each biomaterial depends on the presence and content of different functional groups on its surface [41]. In order to get closer insight into surface properties, determination of acidic and basic sites of both biosorbents was done.

The concentration of total acid and basic sites determined by Boehm method are presented in Table 3.

Table 3 Concentration of acidic and basic active sites on surface of SH and SHM obtained by Boehm method

As can been seen from the obtained results, in SH concentration of total acidic sites is much higher than total basic sites regarding to natural composition of lignocellulosic material. The surface of SH has a higher content of acidic groups, especially phenolic type, which are part of the molecular structure of main components of SH: lignin and cellulose. However, after modification the content of total basic sites in SHM becomes almost ten times larger than in SH, which is in accordance with obtained results from previous section *3.1.3*. Changes which have occurred after alkali treatment indicate that now surface has more oxygen functional groups with basic character.

In order to find which surface modification during alkali treatment of native SH causes biosorption capacity to increase, further research was conducted and SHM was titrated with HCl solution.

Since the carboxylic groups have pKa between 4 and 5 [42], after treatment with 1 M NaOH solution they will be in the basic, sodium salt (-COONa) form. That is the reason why, in

previous experiment, whose results are given in Table 3, they would not react with 0.05 M $NaHCO_3$, but it would react with 0.05 M HCl solution.

In the next set of experiments direct potentiometric titration of SHM with 0.3 M HCl solution was performed. Results shows that for pH change from 7 to 2 (pH range where functional groups with pKa values between 4 and 5 will be practically completely converted from salt to acidic form), after the correction for HCl spent for acidifying the same volume of water from pH 7 to pH 2, there will be used 0.306 ± 0.008 mmol of HCl for 1 g of SHM sample. That is in agreement with above finding that SHM sample practically does not react with $NaHCO_3$, while 1 g of SHM reacts with 0.31 mmol of 0.05 M HCl solution. It can be assumed that SHM functional groups found to be "basic groups" in previous experiment are actually carboxylic groups in sodium salt form.

The complete titration curves of SH and SHM with 0.3 M HCl and NaOH are given in supplementary material (Fig. 1).

3.1.5 FTIR analysis

Figure 4 presents the FTIR-ATR spectrums of SH and SHM with the most significant changes observed. The FTIR spectra of the SH exhibited characteristic peaks for lignocellulosic material that have been reported in our previous work [43]. Peak positions in the FTIR spectrums of both materials are summarized in Table 4.

Fig. 4 *FTIR-ATR spectra of SH and SHM*

The most noticeable change that occurred after alkali treatment was disappearance of carbonyl peak at 1732 cm^{-1} in SHM spectra [44]. This is related to the effect that base has on natural lignocellulosic material: the degradation of hemicellulose. This specific peak characterizes the bonds present in the hemicellulose and hemicellulose-lignin complex, as well as in waxes and fats [45]. Also, from Fig. 4 it can be observed that after alkali treatment, peak at 1233 cm^{-1} has decreased and two new peaks appeared at 1266 and 1227 cm^{-1}. The peak 1233 cm^{-1} is attributed to C-O-C stretching from aryl-alkyl ether linkage [44]. The changes that have occurred in this region could be result of lignin depolymerisation.

Table 4 Peak position in the FTIR-ATR spectrums of SH and SHM

The FTIR-ATR spectrums of SHM before and after metal adsorption are presented in supplementary material (Fig. 4). The noticeable differences, before and after metal adsorption, are in the bands of the O-H stretching (3000–3600 cm^{-1} and 1000-1050 cm^{-1}) as well as in the band of the $-COO^-$ group at about 1580 cm^{-1}, indicating the involvement of –OH and $-COO^-$ groups in adsorption.

3.1.6 Cation exchange capacity (CEC) of SH and SHM

In order to obtain better insight into the bonding mechanism of metals during biosorption process, it is significant to investigate cation exchange capacities (CEC). The net amounts of cations released from both samples are presented in Table 5.

Table 5 Cation exchange capacity for SH and SHM

As can be seen from Table 5 the total CEC (sum of alkali and alkaline-earth ions transferred from the biomass to the aqueous solution) is 6.72 and 29.51 meq/100g for SH and SHM, respectively. Results revealed that alkali treatment enhanced the total CEC almost five times. Also, obtained concentrations of exchangeable cations (except for K^+ ions) are higher in SHM, than in starting sample SH. Apparently, the dominant ion in the exchangeable position in SHM is Na^+, due to treatment with NaOH. Additionally, inorganics that are loosely bonded in lignocellulosic matrix or water-soluble such as potassium can be leached out during modification process, which is also the case here. Since, other inorganics such as calcium and magnesium exists in the hemicellulose of lignocellulosic biomass [52,53] a slight increase of its content in SHM could be due to alkali dissolution of hemicellulose.

Obtained results indicate that these ions (especially Na^+) could be exchanged with other metal ions, through the ion exchange mechanism during the biosorption process.

3.2 Sorption studies

In order to examine the sorption process it is necessary to determine the effects of different operating parameters such as pH, sorbent concentration, metal concentration and contact time. The determination of these parameters is not described in detail in this paper but obtained experimental data are presented in the supplementary materials (Fig. 2).

3.2.1 Kinetic studies

Kinetic models listed in Table 1 were applied to the obtained experimental data (supplementary materials - Fig. 2c) and the kinetic parameters are presented in Table 6.

Table 6 Kinetic parameters for heavy metals sorption by SH and SHM

Considering the excellent values for R^2 (which are close to unit R^2=0.999) obtained from pseudo-second order model and the fact that calculated q_t are very close to the experimental q_{exp} it can be concluded that the sorption of all metals (at specified concentration) onto SH and SHM follows pseudo-second order model. The applicability of this kinetic model indicates that the biosorption of all selected metals involves complexation and ion exchange mechanism [54-56]. The biosorption performance additionally can be determined by calculating the half-life of adsorption process: $t_{1/2} = 1/(k_2 q_t)$ [27]. The parameter $t_{1/2}$ describes how long it takes for the sorbate concentration to decrease to one-half of its initial value. As can be seen from displayed results in Table 6, SHM will approach equilibrium faster than SH. For example the initial concentration of Cu(II) in solution (60 mg/L) will drop by half in 3.2 or 1.4 minutes, depending on the biosorbent used (SH or SHM, respectively).

To exam if the metal ions are being transported within pores of sorbents, experimental data were fitted by Weber-Morris diffusion model. The values of K_{id} and C were calculated from the slope and intercept of the plot (figure not shown) and presented in Table 6. The intercept (C) of the plot indicates the boundary layer effect. The larger it is the greater is involvement of the surface biosorption in the rate-limiting step [57]. As can be seen from Table 6 the values of C are for all metals, higher for SHM than for SH, indicating that the surface biosorption has a significant impact in rate-limiting step. Biosorbent SHM with larger surface and more binding

sites tends to attach more metal ions to the surface of SHM which leads to rapid fall in metal concentration in solution (slowing down the driving force for the mass transfer). According to Šćiban et al. [58] adsorption in most lignocellulosic materials occurs mostly on the surface of the particles, which is in agreement with observation in this paper.

3.2.2 Sorption isotherm models

In this section, obtained data from biosorption experiments with raw and modified material were subject to equilibrium modelling in order to understand the mechanism of biosorption process. Therefore, obtained experimental data were fitted by two-parameter models (Langmuir and Freundlich) and three-parameter Sips isotherm model (models and equations are presented in Table 1). The Langmuir isotherm model [24] assumes: that the surface of sorbent is homogeneous and that the adsorption occurs in monolayer without interactions between sorbed ions. When biosorption is favorable R_L is within 0–1, while for unfavorable, linear and irreversible biosorption $R_L \geq 1$ and $R_L < 0$, respectively [59]. The Freundlich adsorption isotherm [25] model assumes that the surface of sorbent is heterogeneous and the interactions during adsorption occur among adsorbed ions, while the Sips isotherm model [26] combines both of models and it is expected to describe the surface heterogeneity better. When dimensionless factor *s* is between 0 and 1 implies heterogeneity of the system.

Considering obtained results presented in Supplementary materials (Fig. 2), the isotherms were determined for a metal concentration 6 - 120 mg/L for Cu(II) and Zn(II) and 20 – 400 mg/L for Pb(II), at 25 °C for 120 min at pH 5.0. The calculated parameters of isotherm models are summarized in Table 7.

Table 7 Langmuir, Freundlich and Sips isotherm parameters for biosorption of Cu(II), Zn(II) and Pb(II) ions onto SH and SHM

Obviously, significant changes concerning the biosorption capacity have been occurred after alkali treatment of raw material. As can be seen from Table 7 biosorption capacity of SH is 4.83; 5.42 and 24.53 mg/g, while capacity of SHM is 12.25; 8.73 and 46.45 mg/g for Cu(II), Zn(II) and Pb(II) ions, respectively. The difference in binding capacity of Pb(II) ions over the two other

metal ions can be explained by the smaller hydration radius of the lead ions [60] and by the more than three times higher atomic mass of lead. Apparently, alkali treatment improved biosorption capacity of modified material SHM in comparison with starting sample SH. Due to the similar values of R^2 and χ^2 it may be concluded that the adsorption of all metal ions onto SH can be described with both Langmuir and Sips models, indicating monolayer sorption and heterogeneous surface of the SH. However, adsorption onto SHM is described better with Freundlich model except in case of Cu(II), which indicates that multilayer adsorption occurs on the heterogeneous surface of SHM [61,62]. Also, the obtained values of n and R_L confirmed that the biosorption process onto SH and SHM for selected metals, is favourable.

In comparison with other alkali modified lignocellulosic biosorbents from literature, SHM shows higher adsorption capacity for Pb(II) ions than alkali modified: coconut coir fibre (29.41 mg/g) [63], olive stone (15.25 mg/g) [64] and corn cob (7.89 mg/g) [65]. Also, SHM shows higher adsorption capacity for Cu(II) and Zn(II) ions in comparison with alkali modified rice husk (10.9 and 8.14 mg/g, respectively) [66]. According to the results reported in the literature, alkali modified apricot shells could be used as a perspective adsorbent for heavy metals removal from aqueous solution.

3.2.3 Investigation of ion exchange mechanism

Due to higher concentrations of exchangeable cations (especially Na^+) in SHM (Table 5) the involvement of ion-exchange mechanism was investigated following the release of exchangeable cations (K^+, Na^+, Ca^{2+}, Mg^{2+} and H^+ ions) during the biosorption experiments. As a control, the release of cations after soaking the sample in deionized water was measured. These experiments were conducted mixing 0.1 g of samples with 50 mL of metal solution of various concentrations at pH 5.0. The pH value was followed and the concentration of released H^+ ions was determined as described elsewhere [28].

Figure 5 shows the amount of released cations vs. amount of adsorbed metal ions on different metal concentration after the equilibrium was reached. As can be seen from Fig. 5, amount of cations released from SHM is almost equal in comparison to the amount of adsorbed metal ions, suggesting ion exchange mechanism. The EDX spectrums after metal adsorption support this finding (Supplemental material: Fig. 3 and Table 1). Also, Fig. 5 shows that Na^+ ions

are exchanged first, followed by H^+ ions. During the biosorption experiments, decrease of pH value was observed, indicating release of H^+ ions from SHM, which can be explained by surface complexation [67]. This is in agreement with results of kinetic studies.

Fig. 5 *The amount of adsorbed metal ions and relised cations from SHM at different initial metal concentration at T = 25°C, t = 120 min, pH = 5.0)*

3.3 Application of SHM for laboratory wastewater cleaning up

Chemical laboratories generate the wastewaters containing heavy metal ions in low concentrations, which are still above the permitted level to be directly discharged into sewers. In order to show possible practical application of SHM, the drained water originating from atomic adsorption spectrophotometer was chosen. The efficiency of SHM and its suitability for the metal removal from this wastewater was investigated and the obtained results are presented in Table 8.

Table 8 Metal concentration in wastewater before and after treatment with SHM

From the results, it is clear that the SHM is suitable for heavy metals removal from drained water of AAS. After treatment amount of Fe, Pb, Cu, Cr, Ni, and Zn ions were reduced by 97, 87, 81, 80, 33 and 14 %, respectively.

3.4 Desorption study

Regeneration and reuse of exhausted biosorbent is crucial for economically viable and environmentally sustainable process. Disposal of contaminated exhausted biosorbent could become an issue. Therefore, desorption studies are suitable for investigation of capability of biosorbent to be recycled.

In order to investigate the possibility of SHM reusability, desorption and regeneration experiments were performed and the obtained results are presented in Figure 6. As can be seen, desorption efficiency decreased very slowly as the number of cycles increased but still remaining at very high level after each cycle. The results of this study confirm that the biosorbent SHM can

be efficiently recovered by using 0.1 mol/L HCl and as such it is suitable for metal recovery. Successful use of this desorption eluent also indicates that the ion exchange mechanism takes dominant role in adsorption process, due to the intense competition between H^+ and metal ions [39].

After desorption, regenerated biosorbent SHM can be disposed without risk that it contains heavy metals.

Fig. 6 *The desorption efficiency of metal ions after three adsorption/desorption cycles*

4 Conclusions

In this study, for the first time, the usefulness of alkali modified apricot shells (SHM) as a biosorbent for removal of Cu(II), Zn(II) and Pb(II) ions from aqueous solution was investigated. It was found that the treated shells have better adsorption properties than raw sample: adsorption capacity of SH is 4.83; 5.42 and 24.5 mg/g, while capacity of SHM is 12.25; 8.73 and 46.45 mg/g for Cu(II), Zn(II) and Pb(II) ions, respectively.

A characterization study was performed in order to determine the changes of morphological, physical and chemical properties of raw apricot shells during treatment. SEM analysis revealed that alkali treatment enhanced surface roughness providing a larger contact area due to removal of natural fats and waxes. Mercury intrusion porosimetry, confirmed larger surface area and porosity of SHM. Chemical and FTIR analysis showed that alkali treatment induced hemicellulose hydrolysis and lignin depolymerisation, therefore improved the adsorption characteristics of SHM by developing new adsorption sites. Also, the presence of sodium ions as a consequence of alkali treatment (confirmed by EDX analysis), significantly increases the adsorption capacity of SHM by enhanced cation exchange capacity. The results of potentiometric titration and FTIR spectra analysis revealed that after modification of raw material with NaOH, carboxylic groups are in sodium salt form.

Analysis of the cations released during the biosorption shows that the amount of cations released from SHM was almost equal to the amount of adsorbed metal ions indicating ion-excange mechanism. The sodium ions were exchanged first, followed by H^+ and other

exchangeable cations. The applicability of pseudo-second order kinetic model indicates that the heavy metals biosorption involves complexation, too.

Moreover, the SHM could be successfully regenerated with 0.1 mol/L HCl and reused for new biosorption cycle.

Finally, this study revealed that the SHM is suitable biosorbent for cleaning-up drained water of atomic adsorption spectrophotometer.

Acknowledgments

The authors are grateful to the Serbian Ministry of Education, Science and Technological Development for the financial support of this investigation included in the project TR31003 and III43010.

References

[1] J.S. Van Dyk, R. Gama, D. Morrison, S. Swart, B.I. Pletschke, Food processing waste: Problems, current management and prospects for utilisation of the lignocellulose component through enzyme synergistic degradation, Renew. Sust. Energ. Rev. 26 (2013) 521–531.

[2] F.W. Sousa, A.G. Oliveira, J.P. Ribeiro, M.F. Rosa, D. Keukeleire, R.F. Nascimento, Green coconut shell applied as adsorbent for removal of toxic metal ions used fixedbed column technology, J. Environ. Manage. 91 (2010) 1634-1640.

[3] L.H. Velazqez-Jiminez, A. Pavlick, J.R. Rangel-Mendez, Chemical characterization of raw and treated agave bagasse and its potential as adsorbent of metal cations from water, Ind. Crops Prod. 43 (2013) 200-206.

[4] M.N. Rashed, Fruit stones from industrial waste for the removal of lead ions from polluted water, Environ. Monit. Assess. 119 (2006) 31–41.

[5] Z. Lopičić, M. Stojanović, S. Marković, J. Milojković, M. Mihajlović, T. Kaluđerović Radoičić M. Kijevčanin, Effects of different mechanical treatments on structural changes

of lignocellulosic waste biomass and subsequent Cu(II) removal kinetics, Arab J Chem. 2016. https://doi.org/10.1016/j.arabjc.2016.04.005.

[6] J. Petrović, M. Stojanović, J. Milojković, M. Petrović, T. Šoštarić, M. Laušević, M. Mihajlović, Alkali modified hydrochar of grape pomace as a perspective adsorbent of Pb^{2+} from aqueous solution, J. Environ. Manage. 182 (2016) 292-300.

[7] M. Kobya, E. Demirbas, E. Senturk, M. Ince, Adsorption of heavy metal ions from aqueous solutions by activated carbon prepared from apricot stone. Bioresour. Technol. 96 (2005) 1518-1521.

[8] S. Pap, J. Radonić, S. Trifunović, D. Adamović, I. Mihajlović, M. Vojinović Miloradov, M. Turk Sekulić, Evaluation of the adsorption potential of eco-friendly activated carbon prepared from cherry kernels for the removal of Pb^{2+}, Cd^{2+} and Ni^{2+} from aqueous wastes, J. Environ. Manage. 184 (2016) 297-306.

[9] S. Pap, T. Šolević Knudsen, J. Radonić, S. Maletić S.M. Igić, M. Turk Sekulić, Utilization of fruit processing industry waste as green activated carbon for the treatment of heavy metals and chlorophenols contaminated water, J. Clean. Prod. 162 (2017) 958-972.

[10] A. Abdolali, W.S. Guo, H.H. Ngo, S.S. Chen, N.C. Nguyen, K.L. Tung, Typical lignocellulosic wastes and by-products for biosorption process in water and wastewater treatment: a critical review, Bioresour. Technol. 160 (2014) 57–66.

[11] Statistical office of the Republic of Serbia. http://webrzs.stat.gov.rs/WebSite/ 2017 (accessed 22.03.17).

[12] M. Kazemipour, M. Ansari, S. Tajrobehkar, M. Majdzadeh, H.R. Kermani,. Removal of lead, cadmium, zink and copper from industrial wastewater by carbon developed from walnut, hazelnut, almond, pistachio shell and apricot stone, J. Hazard. Mater. 150 (2008) 322-327.

[13] D. Özçimen, Adsorption of copper(II) ions onto hazelnut shell and apricot stone activated carbons, Adsorpt. Sci. Technol. 28 (2010) 327-340.

[14] M. Carrier, A. Loppinet-Serani, D. Denux, J.M. Lasnier, F. Ham-Pichavant, F. Cansell, C. Aymonier, Thermogravimetric analysis as a new method to determine the lignocellulosic composition of biomass. Biomass. Bioenerg. 35 (2011) 298-307.

[15] TAPPI Test Method T222 om-88, Acid-insoluble lignin in wood and pulp. In: Tappi test methods. Atlanta, GA: Technical Association of the Pulp and Paper Industry.

[16] R.C. Pettersen, The chemical composition of wood. In: Rowel, R.M. (Eds.), The Chemistry of Wood. Advances in Chemistry Series 207, American Chemical Society, Washington, DC, USA, 1984, pp. 57-126.

[17] S.K Milonjić, A.L. Ruvarac, M.V. Šušić, The heat of immersion of natural magnetite in aqueous solutions, Termochim. Acta. 11 (1975) 261–266.

[18] H.P. Boehm, Some aspects of the surface chemistry of carbon and other carbons, Carbon. 32 (1994) 759-769.

[19] D.W. Ming, E.R. Allen, C. Galindo, D.L.M. Henninger, Methods for determination cation exchange capacities and compositions of native cations for clinoptilolita, in: Fuentes, G.R., Gonzáles (Eds.), Memories of 3rd International Conference on the Occurrence, Properties and Utilization of Natural Zeolites. Havana, Cuba, 1991, pp. 31-35.

[20] M. Petrović, T. Šoštarić, M. Stojanović, J. Petrović, M. Mihajlović, A. Ćosović, S. Stanković, Mechanism of adsorption of Cu^{2+} and Zn^{2+} on the corn silk (*Zea mays* L.), Ecol. Eng. 99 (2017) 83-90.

[21] S. Lagergren, About the theory of so called adsorption of soluble substances, K. Sven. Veternskapsakad. Handl. 24 (1898) 1-39.

[22] G. Blanchard, M. Maunaye, G. Martin, Removal of heavy metals from waters by means of natural zeolites, Water. Res. 18 (1984) 1501-1507.

[23] W. Weber, J. Morris, Kinetics of adsorption on carbon from solution, J. Sanit. Eng. Div. 89 (1963) 31-60.

[24] L. Langmuir, The adsorption of gases on plane surfaces of glass, mica and platinum, J. Am. Chem. Soc. 40 (1918) 1361–8.

[25] H.M.F. Freundlich, Over the adsorption in solution, J. Phys. Chem. 57 (1906) 385-470.

[26] R. Sips, On the structure of a catalyst surface, J. Chem. Phys. 16 (1948) 490-495.

[27] A.E. Ofomaja, E.B. Naidoo, Biosorption of copper from aqueous solution by chemically activated pine cone: A kinetic study, Chem. Eng. J. 175 (2011) 260-270.

[28] M. Petrović, T. Šoštarić, M. Stojanović, J. Milojković, M. Mihajlović, M. Stanojević, S. Stanković, Removal of Pb^{2+} ions by raw Corn silk *(Zea Mays* L. *)* as a novel biosorbent, J. Taiwan. Inst. Chem. Eng. 58 (2016) 407-416.

[29] B. Xiao, X.F. Sun, C.S. Run, Chemical, structural, and thermal characterizations of alkali-soluble lignins and hemicelluloses, and cellulose from maize stems, rye straw, and rice straw, Polym. Degrad. Stabil. 74 (2001) 307–319.

[30] A.E.O. Ben Sghaier, Y. Chaabouni, F. Sakli, Morphological and crystalline characterization of NaOH and NaOCl treated *Agave americana* L. fiber, Ind. Crop. Prod. 36 (2012) 257-266.

[31] K.W. Lin, M.R. Ladisch, M. Voloch, J.A. Patterson, C.H. Noller, Effect of pretreatment and fermentation on pore size in cellulosic materials, Biotechnol. Bioeng. 27 (1985) 1427-1433.

[32] I. Demiral, S.C. Kul, Pyrolysis of apricot kernel shell in fixed-bed reactor: characterization of bio-oil and char, J. Anal. Appl. Pyrolysis. 107 (2014) 17-24.

[33] J. Vadiveloo, B. Nurfariza, J. G. Fadel, Nutritional improvement of rice husks, Anim. Feed Sci. Technol. 151 (2009) 299–305.

[34] Y. Sun, J. Cheng, Hydrolysis of lignocellulosic materials for ethanol production: a review, Bioresour. Technol. 83 (2002) 1-11.

[35] F. Asadi, H. Shariatmadari, N. Mirghaffari, Modification of rice hull and sawdust sorptive characteristics for remove heavy metals from synthetic solutions and wastewater, J. Hazard. Mater. 154 (2008) 451-458.

[36] B.S. Ndazi, S. Karlsson, J.V. Tesha, C.W. Nyahumwa, Chemical and physical modifications of rice husks for use as composite panels, Compos. Part. A. Appl. Sci. Manuf. 38 (2007) 925–935.

[37] E. M. Ciannamea, P.M. Stefani, R. A. Ruseckaite, Medium-density particleboards from modified rice husks and soybean protein concentrate-based adhesives, Bioresour. Technol. 101 (2010) 818–825.

[38] M. Calero, A. Pérez, G. Blázquez, A. Ronda, M.A. Martín-Lara, Characterization of chemically modified biosorbents from olive tree pruning for the biosorption of lead, Ecol. Eng. 58 (2013) 344-354.

[39] I. Anastopoulos, M. Panagiotou, C. Ehaliotis, P. Tarantilis, I. Massas, NaOH pretreatment of compost derived from olive tree pruning waste biomass greatly improves biosorbent characteristics for the removal of Pb^{2+} and Ni^{2+} from aqueous solutions. Chem. Ecol. 31 (2015) 724-740.

[40] N. Fiol, I. Villaescusa, Determination of sorbent point zero charge: usefulness in sorption studies, Environ. Chem. Lett. 7 (2009) 79 – 84.

[41] G. Blazquez, M.A. Martın-Lara, E. Dionisio-Ruiz, G. Tenorio, M. Calero, Copper biosorption by pine cone shell and thermal decomposition study of the exhausted biosorbent, J. Ind. Eng. Chem. 18 (2012) 1741–1750.

[42] M.B. Smith, J. March, March's Advanced Organic Chemistry, Fifth edition, John Willey and sons, inc., USA, 2001.

[43] T. Šoštarić, M. Petrović, J. Milojković, Č. Lačnjevac, A. Ćosović, M. Stanojević, M. Stojanović, Application of waste apricot stones from fruit processing industry in environmental clean-up: copper biosorption study, Fruits. 70 (2015) 271-280.

[44] H. Yang, R. Yan, H. Chen, D.H. Lee, Characteristics of hemicellulose, cellulose and lignin pyrolysis, Fuel. 86 (2007) 1781–1788.

[45] S.P.S. Chundawat, B. Venkatesh, B.E. Dale, Effect of Particle Size Based Separation of Milled Corn Stover on AFEX Pretreatment and Enzymatic Digestibility, Biotechnol. Bioeng. 96 (2007) 219–231.

[46] E. Pehlivan, T. Altun, S. Cetin, B.M. Iqbal, Lead sorption by waste biomass of hazelnut and almond shell, J. Hazard. Mater. 167 (2009) 1203–1208.

[47] E. Pretsch, P. Bühlmann, M. Badertscher, Structure Determination of Organic Compounds Tables of Spectral Data, Fourth Edition, Springer-Verlag, Germany, 2009, p-64.

[48] O. Faix, Classification of Lignins from Different Botanical Origins by FT-IR Spectroscopy, Holzforschung. 45 (1991) 21-27.

[49] M. Martinez, N. Miralles, S. Hidalgo, N. Fiol, I. Villaescusa, J. Poch, Removal of lead(II) and cadmium(II) from aqueous solutions using grape stalk waste, J. Hazard. Mater. 133 (2006) 203-211.

[50] M. Poletto, V. Pistor, A.J. Zattera, Structural Characteristics and Thermal Properties of Native Cellulose. In: Van de Ven T., GodboutL. (Eds) Cellulose – Fundamental Aspects. In Tech. 2013. https://doi:10.5772/50452.

[51] I.A. Aguayo-Villarreal, L.A. Ramírez-Montoya, V. Hernández-Montoya, A. Bonilla-Petriciolet, M.A. Montes-Morán, E.M. Ramírez-López, Sorption mechanism of anionic dyes on pecan nut shells (*Carya illinoinensis*) using batch and continuous systems, Ind. Crop. Prod. 48 (2013) 89-97.

[52] T.R. Miles, T.R.Jr. Miles, L.L. Baxter, R.W. Bryers, B.M. Jenkins, L.L. Oden, Boiler deposits from firing biomass fuels, Biomass. Bioenerg. 10 (1996) 125-138.

[53] M.T. Reza, J.G. Lynam, H.M. Uddin, C.J. Coronella, Hydrothermal carbonization: Fate of inorganics, Biomass. Bioenerg. 49 (2013) 86-94.

[54] V. Padmavathy, P. Vasudevan, S.C. Dhingra, Biosorption of Nickel(II) ions on bakers yeast, Process. Biochem 38 (2003) 1389–95.

[55] L. Zhong, X. Peng, D. Yang, R. Sun, Adsorption of heavy metals by a porous bioadsorbent from lignocellulosic biomass reconstructed in anionic liquid, J. Agric. Food. Chem. 60 (2012) 5621–8.

[56] X.K. OuYang, R.N. Jin, L.P. Yang, Z.S. Wen, L.Y. Yang, Y.G. Wang, C.Y. Wang, Partially hydroliyzed Bamboo (*Phyllostachys heterocycla*) as a porous bioadsorbent for the removal of Pb(II) from aqueous mixtures, J. Agric. Food. Chem. 62 (2014) 6007–15.

[57] A.E. Ofomaja, E.B. Naidoo, S.J. Modise, Kinetic and pseudo-second-order modelling of lead biosorption onto pine cone powder, Ind. Eng. Chem. Res. 49 (2010) 2562-2572.

[58] M. Šćiban, M. Klašnja, B. Škrbić, Adsorption of copper ions from water by modified agricultural by-products, Desalination 229 (2008) 170-180.

[59] G. Yuvaraja, N. Krishnaiah, M.V. Subbaiah, A. Krishnaiah, Biosorption of Pb(II) from aqueous solution by *Solanum melongena* leaf powder as a low-cost biosorbent prepared from agricultural waste, Colloid. Surface. B. 114 (2014) 75-81.

[60] E. R. Nightingale Jr., Phenomenological theory of ion solvation, Effective radii of hydrated ions, J. Phys. Chem. 63 (1959) 1381–1387.

[61] G. Crini, P.M. Badot, Application of chitosan, a natural aminopolysaccharide, for dye removal from aqueous solutions by adsorption processes using batch studies: a review of recent literature, Prog. Polym. Sci. 33 (2008) 399–447.

[62] T. Song, J. Liang, X. Bai, Y. Li, Y. Wei, S. Huang, L. Dong, J. Qu, Y. Jin, Biosorption of cadmium ions from aqueous solution by modified *Auricularia Auricula* matrix waste, J. Mol. Liq. 241 (2017) 1023-1031.

[63] P.M. Shukla, S.R. Shukla, Biosorption of Cu(II), Pb(II), Ni(II), and Fe(II) on alkali treated coir fibers, Sep. Sci. Technol. 48 (2013) 421-428.

[64] G. Blázquez, M. Calero, A. Ronda, G. Tenorio, M.A. Martín-Lara, Study of kinetics in the biosorption of lead onto native and chemically treated olive stone, J. Ind. Eng. Chem. 20, (2014) 2754-2760.

[65] G. Tan, H. Yuan, Y. Liu, D. Xiao, Removal of lead from aqueous solution with native and chemically modified corn cobs, J. Hazard. Mater. 174 (2010) 740–5.

[66] K.K. Krishnani, X. Meng, C. Christodoulatos, V.M. Boddu, Biosorption mechanism of nine different heavy metals onto biomatrix from rice husk, J. Hazard. Mater. 153 (2008) 1222–1234.

[67] H. Chen, G. Dai, J. Zhao, A. Zhong, J. Wu, H. Yan, Removal of copper(II) ions by a biosorbent – *Cinnamomum camphora* leaves powder, J. Hazard. Mater. 177 (2010) 228-236.

Table 1

Models used for evaluation of heavy metals sorption onto SH and SHM

Model	Equation	Parameter	Reference
Isotherm model			
Langmuir	$q_e = \frac{q_{max} K_L C_e}{1+K_L C_e}$ $R_L = \frac{1}{(1+K_L C_0)}$	q_e (mg/g): sorption capacity at equilibrium q_{max} (mg/g): maximum sorption capacity K_L (L/mg): Langmuir constant C_e (mg/L): equilibrium concentration R_L: dimension less separation factor C_o (mg/L) - the highest initial metal concentration	[24]
Freundlich	$q_e = K_f \, C_e^{1/n}$	K_f (mg/g)(L/mg)$^{1/n}$: Freundlich constant *n:* heterogeneity factor	[25]
Sips	$q_e = \frac{q_{max} K_s C_e^s}{1+ C_e K_s^s}$	K_s (L/g): Sips constant *s*: heterogeneity factor	[26]
Kinetic model			
Pseudo-first order	$q_t = q_e\left(1 - e^{-k_1 t}\right)$	q_t (mg/g): sorption capacity at time *t* k_1 (1/min): the pseudo-first order rate constant	[21]
Pseudo-second order	$q_t = \frac{t}{\left(1/k_2 q_e^2\right)+\left(1/q_e\right)}$	k_2 (g/mg/min): the pseudo-second order rate constant	[22]
	$t_{1/2} = 1/k_2 \, q_t$	$t_{1/2}$ (min): half-life of adsorption process	[27]
Intra-particle diffusion model	$q = K_{id} t^{0.5} + C$	K_{id} (mg/(min$^{1/2}$g)): the intra-particle diffusion parameter *C* (mg/g): intercept	[23]

Table 2

Physical and chemical properties of SH and SHM

		SH	SHM
	Dry matter (%)	92.39 ± 1.76	93.64 ± 1.78
	Moisture (%)	7.30 ± 0.13	4.50 ± 0.08
	Ash (%)	1.02 ± 0.03	1.76 ± 0.05
Structural composition	Acetone soluble compounds (%)	2.56 ± 0.04	1.41 ± 0.02
	Lignin (%)	22.72 ± 0.34	21.21 ± 0.32
	Holocellulose (%)	74.46 ± 1.12	60.75 ± 0.91
	Hemicellulose (%)	19.23 ±0.29	3.52 ± 0.05
	Cellulose (%)	55.23 ± 0.83	57.23 ± 0.86
Elemental analysis	C (%)	47.6 ± 1.9	46.1 ± 1.8
	H (%)	6.24 ± 0.12	6.52 ± 0.13
	N (%)	0.12 ± 0.01	<0.1
	S (%)	-	-
	O (from difference) (%)	46.03 ± 2.03	47.43 ± 1.94
Surface properties	Accessible porosity (%)	24.7 ± 0.5	29.9 ± 0.6
	Total pore volume (mm^3/g)	218 ± 11	271 ± 14
	Specific surface area (m^2/g)	15.4 ± 0.8	20.0 ± 1.0
	Average pore diameter (nm)	393 ± 10	468 ± 10
Density	Bulk density (g/cm^3)	1.15 ± 0.05	1.10 ± 0.05
	Apparent density (g/cm^3)	1.50 ± 0.05	1.58 ± 0.05
	Loss of biomass (%)	-	16

Table 3

Concentration of acidic and basic active sites on surface of SH and SHM obtained by Boehm method

	Total acidic sites (mmol/g)	Carboxylic (mmol/g)	Lactonic (mmol/g)	Phenolic (mmol/g)	Basic sites (mmol/g)
SH	1.62 ± 0.02	0.02 ± 0.02	0.46 ± 0.03	1.14 ± 0.03	0.04 ± 0.02
SHM	0.36 ± 0.02	-0.01 ± 0.02	0.19 ± 0.03	0.18 ± 0.03	0.31 ± 0.02

Table 4

Peak position in the FTIR-ATR spectrums of SH and SHM

Wavenumber (cm^{-1})			
SH	SHM	Functional groups	Refs.
3347	3333	OH stretching	[46]
2923	2897	C-H_n stretching	[46]
1732	-	C=O stretching	[46]
1639	-	C=C	[46]
1593	1592	COO^-	[47]
1504	1504	C=C stretching	[48, 49]
1459	1458	OH bending	[38]
1421	1420	COO^-	[47]
1372	1368	CH bending	[50]
1327	1323	CH bending	[50]
	1266	C-O stretching	[51]
1233	1227	C-O-C stretching	[44]
1155	1158	C-O-C stretching	[38]
1105	1105	OH association	[38]
1031	1027	C-O stretching and C-O deformation	[38]

Table 5

Cation exchange capacity for SH and SHM

	Na^+	K^+	Ca^{2+}	Mg^{2+}	∑
	meq/100g	meq/100g	meq/100g	meq/100g	meq/100g
SH	4.03 ± 0.15	0.48 ± 0.02	0.80 ± 0.06	1.41 ± 0.09	6.72 ± 0.32
SHM	25.4 ± 0.9	0.22 ± 0.01	2.29 ± 0.16	1.60 ± 0.11	29.51 ± 1.18

Table 6

Kinetic parameters for heavy metals sorption by SH and SHM

	Adsorbent					
	SH			SHM		
	Cu	Zn	Pb	Cu	Zn	Pb
q_{exp} (mg/g)	5.00	4.18	22.90	9.73	9.00	37.37
Pseudo-first order model						
q_t (mg/g)	4.52	4.09	23.96	9.31	8.87	36.56
k_1 (1/min)	0.942	0.821	2.015	0.515	0.577	0.136
R^2	0.867	0.959	0.992	0.909	0.978	0.919
Pseudo-second order model						
q_t (mg/g)	5.01	4.14	22.85	9.70	9.04	37.35
k_2 (g/mg/min)	0.062	0.278	0.048	0.071	0.141	0.050
R^2	0.999	0.999	0.999	0.999	0.999	0.999
$k_2 q_t$ (1/min)	0.310	1.151	1.097	0.689	1.275	1.867
$t_{1/2}$ (min)	3.219	0.869	0.912	1.452	0.784	0.535
Weber-Morris diffusion model						
K_{id1} (mg/(min$^{1/2}$g))	0.254	0.334	5.530	0.468	1.251	5.032
C (mg/g)	2.892	2.530	4.276	6.979	4.644	24.03
R^2	0.997	0.999	0.995	0.988	0.997	0.973
K_{id2} (mg/(min$^{1/2}$g))	0.102	0.003	0.089	0.087	0.057	0.253
C (mg/g)	3.859	4.067	21.82	8.714	8.426	34.82
R^2	0.870	0.836	0.594	0.939	0.939	0.865

Table 7

Langmuir, Freundlich and Sips isotherm parameters for biosorption of Cu(II), Zn(II) and Pb(II) ions onto SH and SHM

		SH			SHM		
		Cu	Zn	Pb	Cu	Zn	Pb
Langmuir	q_m (mg/g)	4.24	5.06	22.19	8.99	8.65	33.39
	K_L (L/mg)	0.162	0.067	0.110	0.738	5.365	0.283
	R_L	0.152	0.459	0.305	0.213	0.036	0.046
	R^2	0.976	0.973	0.849	0.929	0.776	0.871
	χ^2	0.009	0.011	8.455	0.060	1.839	3.246
Freundlich	K_f (mg/g)(L/mg)$^{1/n}$	0.178	1.196	8.098	6.123	4.835	18.95
	1/n	0.183	0.299	0.177	0.089	0.130	0.109
	R^2	0.965	0.960	0.796	0.988	0.964	0.971
	χ^2	0.014	0.016	11.42	0.010	0.374	0.722
Sips	q_m (mg/g)	4.83	5.42	24.53	12.25	8.73	46.45
	K_s (L/g)	0.279	0.087	0.205	0.884	0.070	0.540
	s	0.638	0.864	0.659	0.261	0.171	0.302
	R^2	0.987	0.974	0.887	0.994	0.854	0.851
	χ^2	0.007	0.016	9.461	0.007	0.477	18.70

Table 8

Metal concentration in wastewater before and after treatment with SHM

	Metal concentration (mg/L)					
	Cu	Zn	Fe	Pb	Ni	Cr
WW before treatment	0.490	0.662	3.340	15.9	0.120	0.100
WW after treatment	0.094	0.572	0.108	2.02	0.080	0.020
Percentage of removal	81%	14%	97%	87%	33%	80%

Highlights

- Biosorption of heavy metals on raw and alkali treated apricot shells was studied.
- Alkali activation significantly improves adsorption properties of raw sample.
- Biosorption mechanism is ion-exchange followed by heavy metals complexation.
- Based on desorption study results, biosorbent can be efficiently recovered and reused.
- The developed biosorbent was successfully applied on real sample.

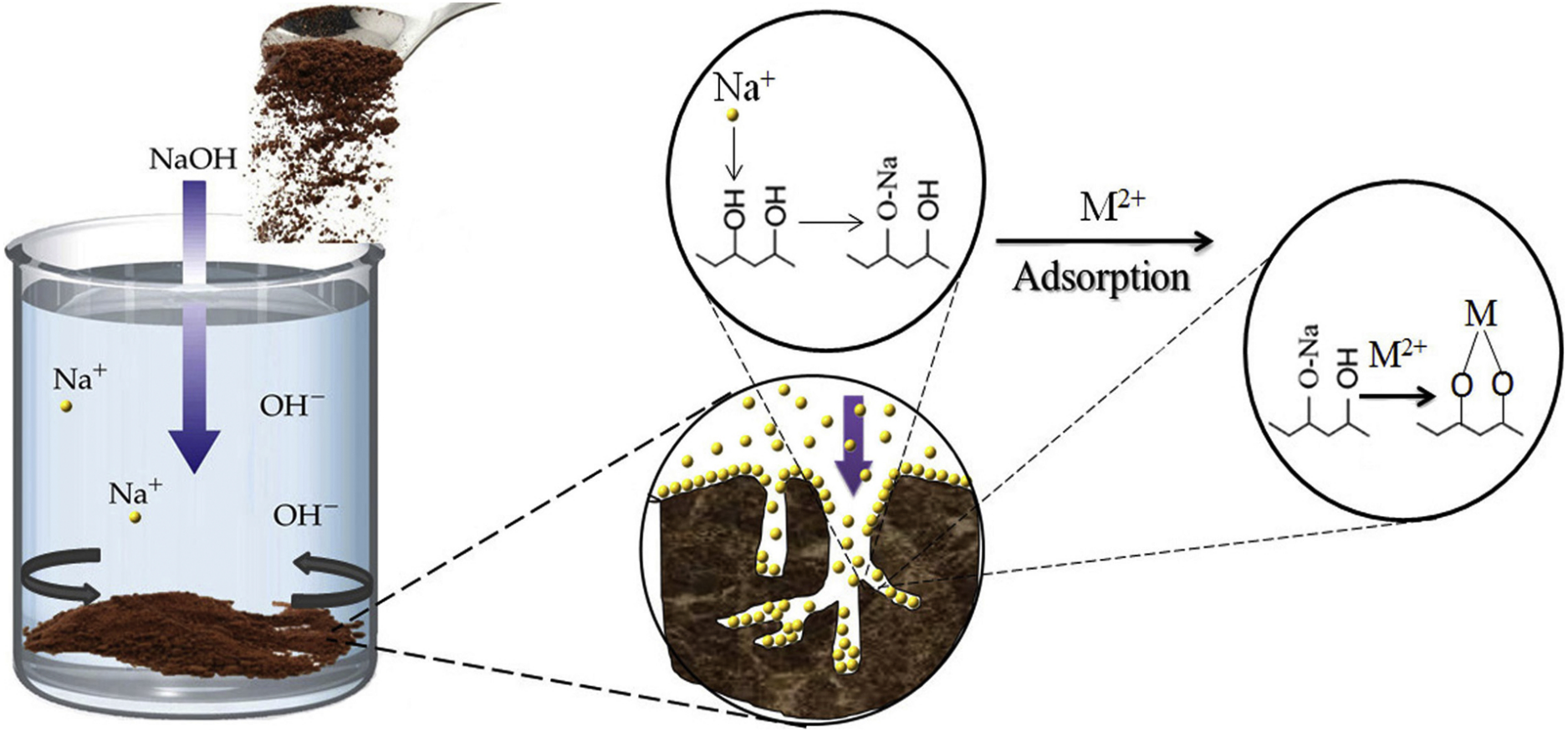

Graphics Abstract

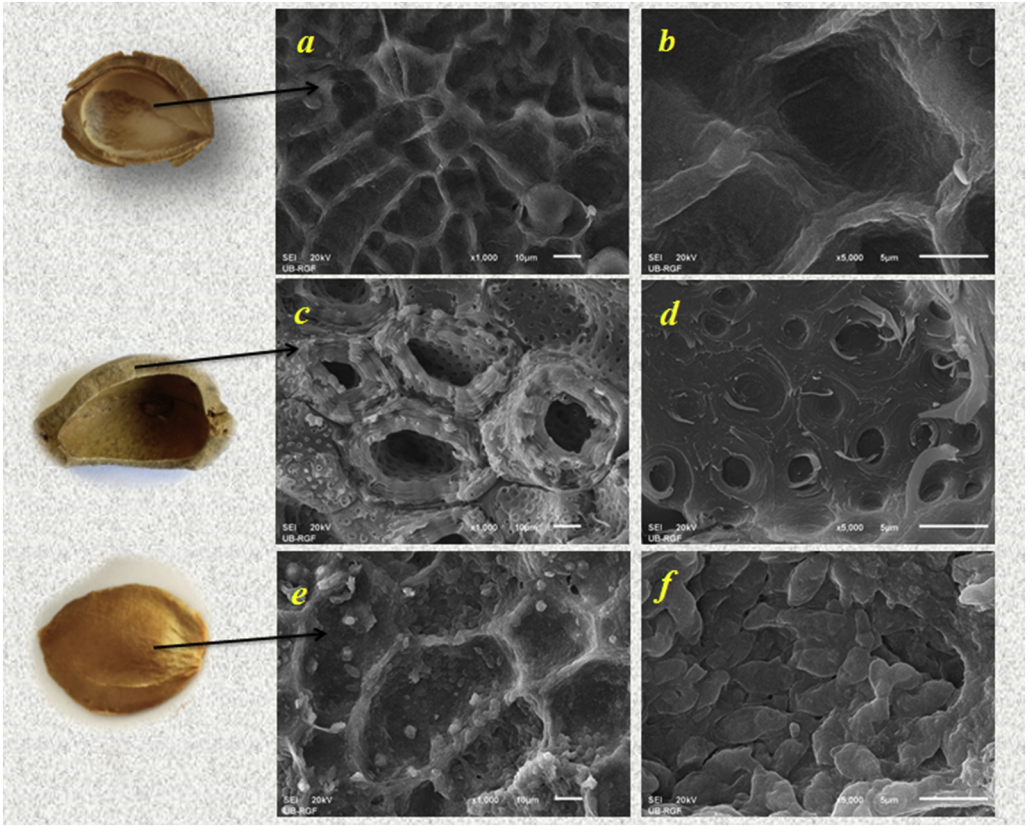

Figure 1

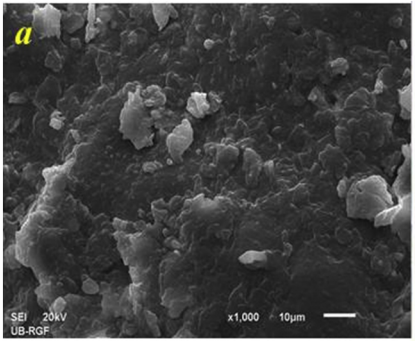
a
SEI 20kV
UB-RGF
x1,000 10µm

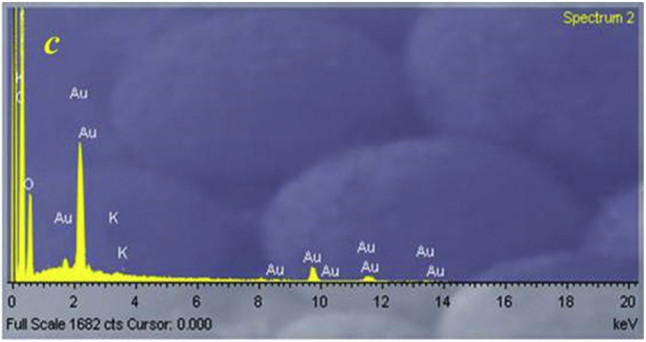
c
Spectrum 2
O
Au
Au
Au
K
K
Au
Au
Au
Au
Au
Au
Au
0 2 4 6 8 10 12 14 16 18 20
Full Scale 1682 cts Cursor: 0.000
keV

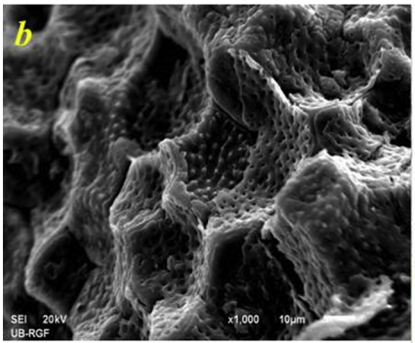
b
SEI 20kV
UB-RGF
x1,000 10µm

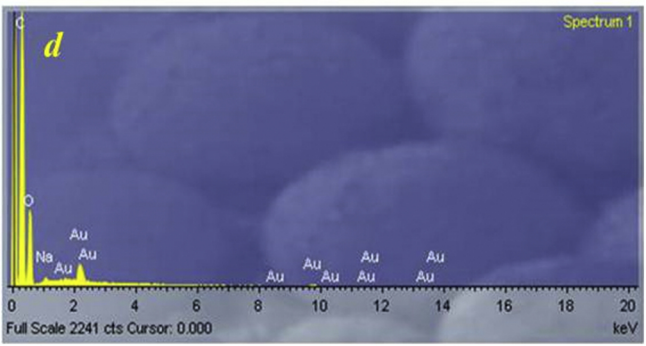
d
Spectrum 1
O
Na
Au
Au
Au
Au
Au
Au
Au
Au
Au
Au
0 2 4 6 8 10 12 14 16 18 20
Full Scale 2241 cts Cursor: 0.000
keV

Figure 2

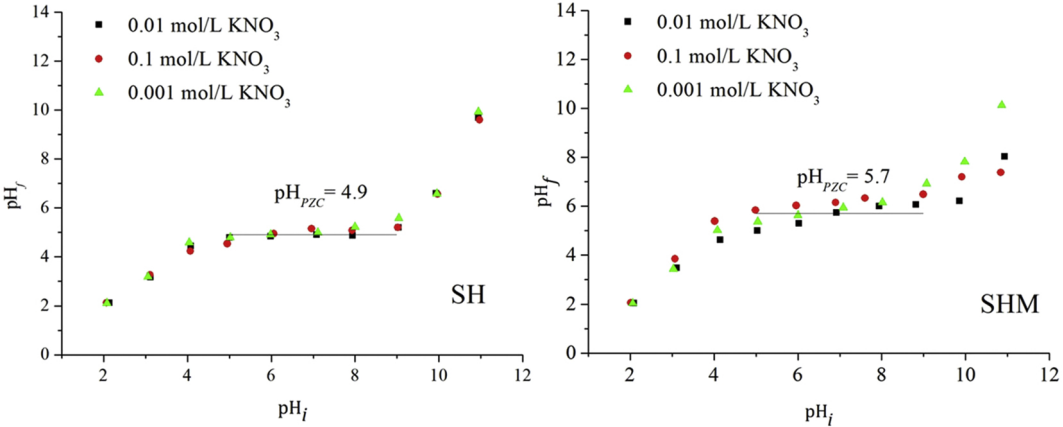
0.01 mol/L KNO3
0.1 mol/L KNO3
0.001 mol/L KNO3
pHPZC = 4.9
SH
pHf
pHi
0.01 mol/L KNO3
0.1 mol/L KNO3
0.001 mol/L KNO3
pHPZC = 5.7
SHM
pHf
pHi

Figure 3

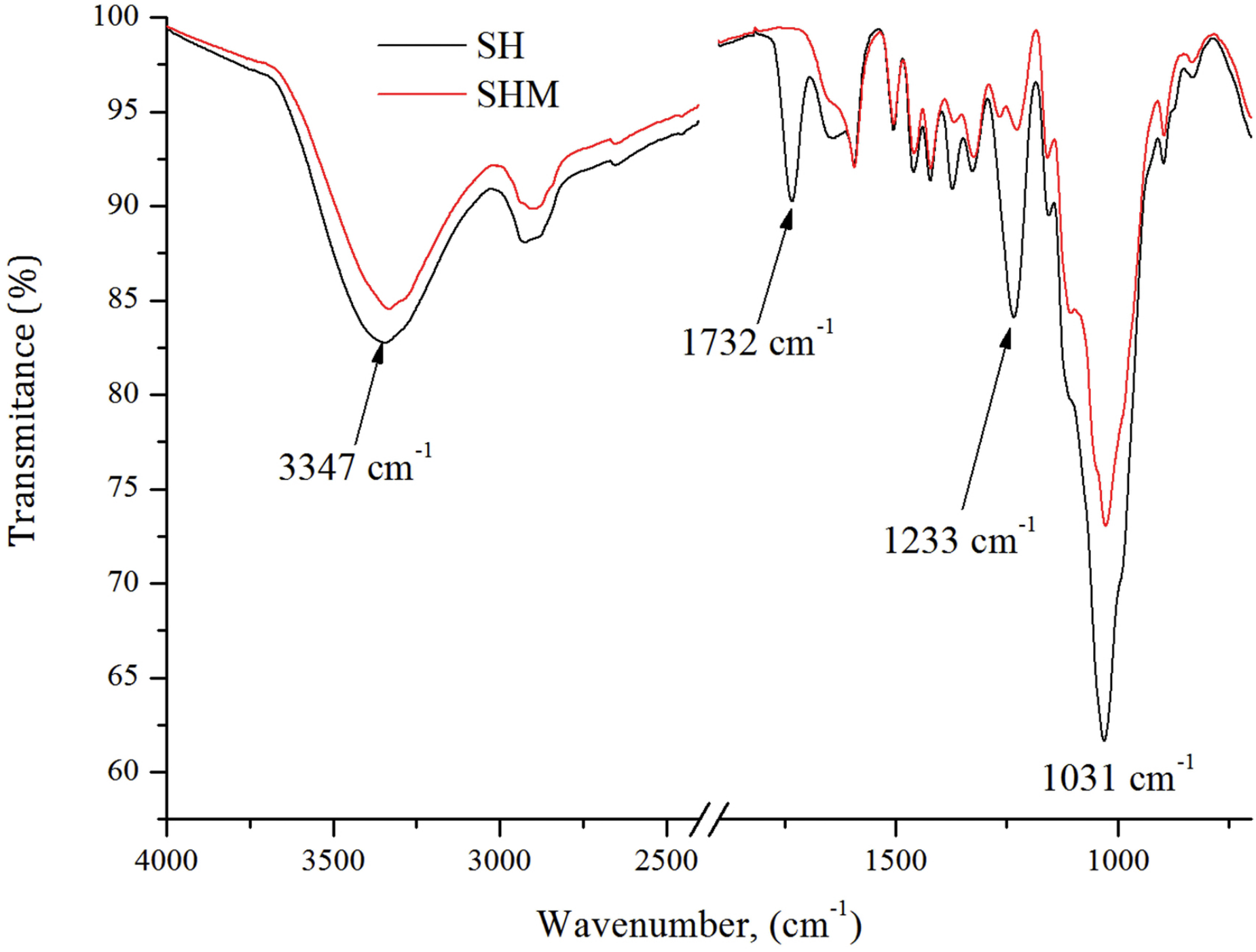
SH
SHM
Transmitance (%)
100
95
90
85
80
75
70
65
60
3347 cm-1
1732 cm-1
1233 cm-1
1031 cm-1
4000
3500
3000
2500
1500
1000
Wavenumber, (cm-1)

Figure 4

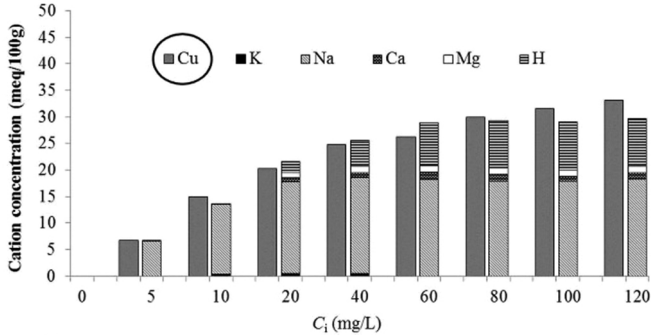
Cu
K
Na
Ca
Mg
H
Cation concentration (meq/100g)
C_i (mg/L)

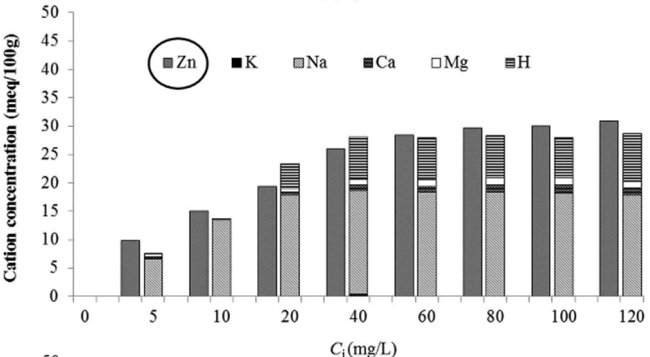
Zn
K
Na
Ca
Mg
H
Cation concentration (meq/100g)
C_i (mg/L)

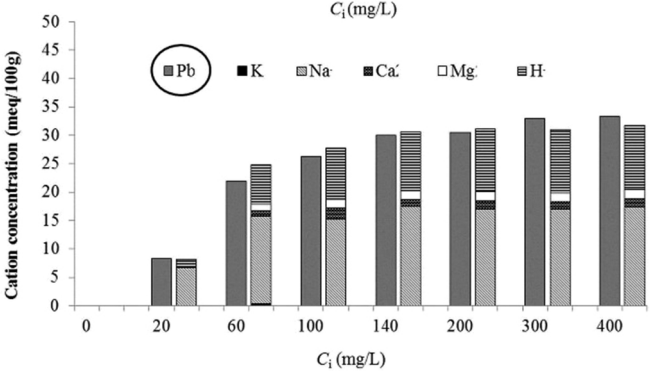
Pb
K
Na
Ca
Mg
H
Cation concentration (meq/100g)
C_i (mg/L)

Figure 5

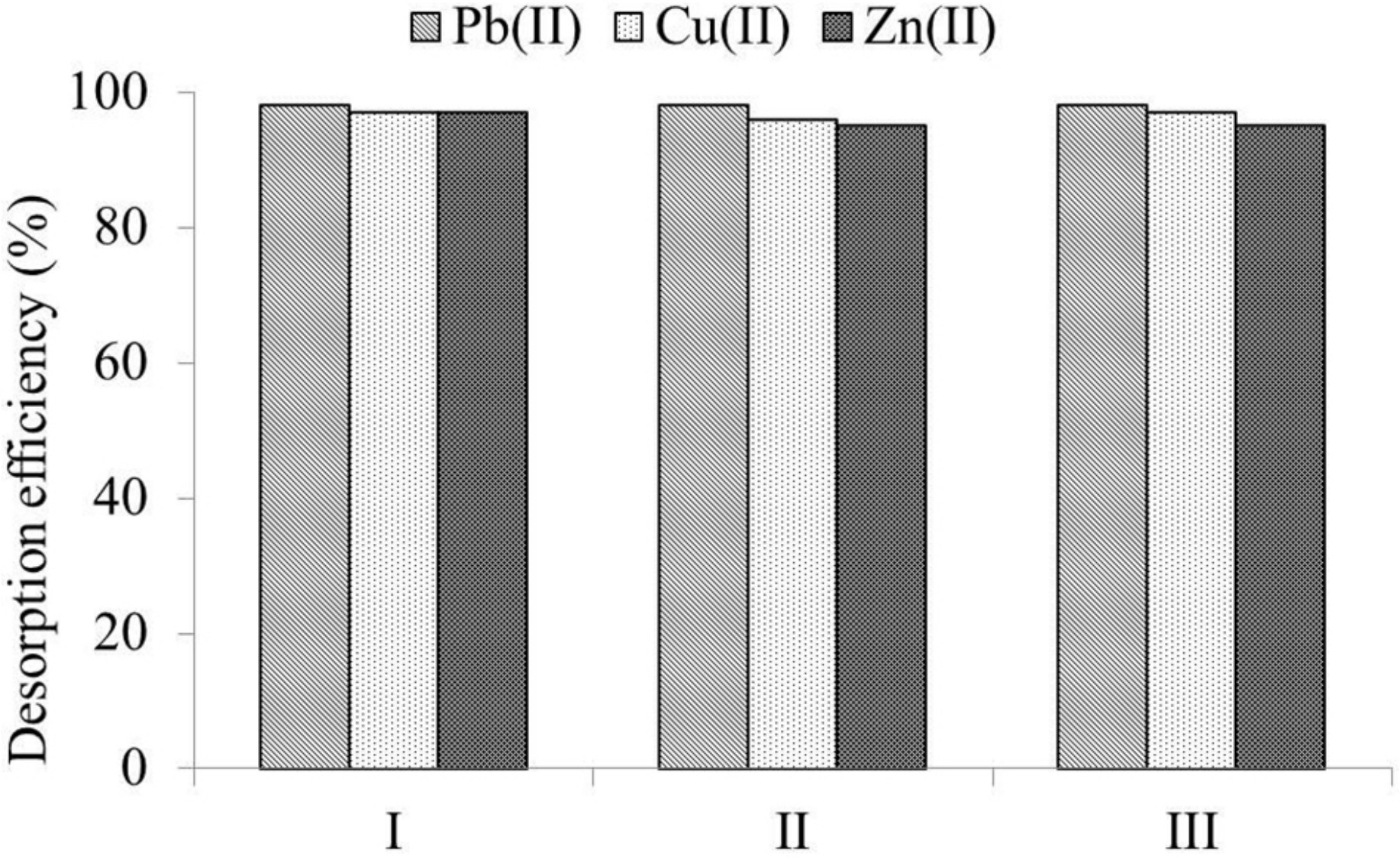
Pb(II)
Cu(II)
Zn(II)
Desorption efficiency (%)
100
80
60
40
20
0
I
II
III

Figure 6